

---

# Entropy Controlled Non-Stationarity for Improving Performance of Independent Learners in Anonymous MARL Settings

---

Tanvi Verma Pradeep Varakantham Hoong Chuin Lau

School of Information Systems, Singapore Management University, Singapore

tanviverma.2015@phdis.smu.edu.sg, pradeepv@smu.edu.sg, hclau@smu.edu.sg

## Abstract

With the advent of sequential matching (of supply and demand) systems (uber, Lyft, Grab for taxis; ubereats, deliveroo, etc for food; amazon prime, lazada etc. for groceries) across many online and offline services, individuals (taxi drivers, delivery boys, delivery van drivers, etc.) earn more by being at the "right" place at the "right" time. We focus on learning techniques for providing guidance (on right locations to be at right times) to individuals in the presence of other "learning" individuals. Interactions between individuals are anonymous, i.e, the outcome of an interaction (competing for demand) is independent of the identity of the agents and therefore we refer to these as Anonymous MARL settings.

Existing research of relevance is on independent learning using Reinforcement Learning (RL) or on Multi-Agent Reinforcement Learning (MARL). The number of individuals in aggregation systems is extremely large and individuals have their own selfish interest (of maximising revenue). Therefore, traditional MARL approaches are either not scalable or assumptions of common objective or action coordination are not viable. In this paper, we focus on improving performance of independent reinforcement learners, specifically the popular Deep Q-Networks (DQN) and Advantage Actor Critic (A2C) approaches by exploiting anonymity. Specifically, we control non-stationarity introduced by other agents using entropy of agent density distribution. We demonstrate a significant improvement in revenue for individuals and for all agents together with our learners on a generic experimental set up for aggregation systems and a real world taxi dataset.

## 1 Introduction

Systems that aggregate supply to ensure a better matching of demand and supply have significantly improved performance metrics in taxi services, food delivery, grocery delivery and other such online to offline services. These systems continuously and sequentially match available supply with demand. For the individuals (taxi drivers, delivery boys, delivery van drivers) that are responsible for supply, learning to be at the "right" place at the "right" time is essential to maximizing their revenue. This learning problem is challenging because of the uncertainty about demand (which will determine the revenue earned) and the locations of other "learning" individuals (which will determine whether the demand is assigned to the current individual).

Given the presence of multiple selfish learning agents, a key focus area of relevance is Multi-Agent Reinforcement Learning (MARL) [Tan, 1993; Busoniu et al., 2008], where multiple agents are learning to maximize their individual rewards. There are two main issues with such an approach in case of sequential matching problems of interest: (a) The definition of fairness when learning for multiple agents is unclear as the agent actions may or may not be synchronised. Furthermore, agents can have different starting beliefs and demand is dynamic or non-stationary. (b) The scale of matching problems is typically very large (e.g., 40000 taxis in a small city like Singapore) and hence computing policies for all agents is computationally very challenging.

An orthogonal thread of MARL has focussed on teams of agents that maximize the global reward [Perolat et al., 2017; Nguyen et al., 2017b] or agents cooperate to achieve a common goal [Hausknecht and Stone, 2015; Foerster et al., 2016]. The learning approaches there are also limited in scalability with respect to number of agents or types of agents. The problems of interest in this paper are focussed on individual agents that are maximizing their own revenue rather than a team revenue. Therefore,

existing MARL approaches are not suitable for the problem and hence we focus on improving performance of independent learners (ILs) in this paper.

Existing work [Verma et al., 2017] in multi-agent sequential matching problems has employed Reinforcement Learning (RL) for each individual to learn a decision making policy. However, this line of work has assumed that other agents employ stationary and fixed strategies, rather than adaptive strategies. Due to the non-stationarity introduced when multiple agents learn independently, the performance of traditional table based Q-learning approaches is extremely poor.

The use of deep neural networks (instead of table based representations) has become hugely popular in the reinforcement learning community [Mnih et al., 2015; Silver et al., 2017]. Policy gradient methods and Q-learning methods have been successfully used with deep neural networks to improve accuracy and scalability. In this paper, we improve the leading independent RL methods, specifically DQN (Deep Q-Networks) and A2C (Advantage Actor Critic) specifically for MSMPs:

- Extending on past work on interaction anonymity in multi-agent planning under uncertainty [Varakantham et al., 2012, 2014; Nguyen et al., 2017a], we describe the notion of interaction anonymity in the context of multi-agent reinforcement learning.
- We then provide mechanisms to exploit interaction anonymity in independent learning by extending the well known DQN (Deep Q-Network) and A2C (Advantage Actor-Critic) methods. Specifically, we aim to predict and control the non-stationarity introduced by other agents by finding policies that maximize (or minimize) the entropy on agent state distribution.
- To demonstrate the utility of our approaches, we performed extensive experiments on a synthetic data set (that is representative of multiple multi-agent sequential matching problems) and a real taxi data set. We observe that our individual learners based on DQN and A2C are able to learn policies that are fair (minor differences in individual values) and most importantly, the individual and joint (social welfare) values of the learning agents are significantly higher than existing benchmarks.

## 2 Motivating Problems

This paper is motivated by problems where there are multiple agents and matching of agents to customer demand is done on a continuous basis. We refer to these problems as Multi-Agent Sequential Matching Problems (MSMPs) and our focus is on enabling individual agents to learn effectively and efficiently. While there are many such

domains, here we provide three MSMPs:

**Taxi Aggregation:** Companies like Uber, Lyft, Didi, Grab etc. all provide taxi supply aggregation systems. The goal is to ensure wait times for customers is minimal or amount of revenue earned is maximized by matching taxi drivers to customers on a regular basis. However, these goals of the aggregation companies may not be correlated to the individual driver objective of maximizing their own revenue. The methods provided in this paper will be used to guide individual drivers to "right" locations at "right" times based on their past experiences of customer demand and taxi supply (obtained directly/indirectly from the aggregation company), while also considering that other drivers are learning simultaneously to improve their revenue.

**Food or Grocery Delivery:** Aggregation systems have also become very popular for food delivery (Deliveroo, UberEats, Foodpanda, DoorDash etc.) and grocery delivery (AmazonFresh, Deliv, RedMart etc.) services. They offer access to multiple restaurants/grocery stores to the customers and use services of delivery boys/delivery vans to deliver the food/grocery. Similar to taxi aggregation systems, our work can be used to guide delivery boy/van to be present at right locations at right times so as to improve their individual revenue.

**Supply Aggregation in Logistics:** More and more online buyers now prefer same day delivery services and traditional logistic companies which maximize usage of trucks, drivers and other resources are not suitable for it. Companies like Amazon Flex, Postmates, Hitch etc. connect shippers with travellers/courier personnels to serve same day/on-demand delivery requests. The courier personnels in this system can employ the proposed method to learn to be at "right" place at "right" time by learning from the past experiences.

## 3 Background: Reinforcement Learning (RL)

In this section, we briefly describe the Reinforcement Learning (RL) problem and leading approaches (of relevance to this paper) for solving large scale RL problems.

The RL problem for an agent is to maximize the long run reward while operating in an environment represented as a Markov Decision Process (MDP). Formally, an MDP is represented by the tuple  $\langle S, A, T, R \rangle$ , where  $S$  is the set of states encountered by the agent,  $A$  is the set of actions,  $T(s, a, s')$  represents the probability of transitioning from state  $s$  to state  $s'$  on taking action  $a$  and  $R(s, a)$  represents the reward obtained on taking action  $a$  in state  $s$ . The RL problem is to learn a policy that maximizes the

long term reward while only obtaining experiences (and not knowing the full reward,  $R$  and transition,  $T$  models) of transitions and reinforcements. An experience is defined as  $(s, a, s', r)$  and typically there is an episode of experiences that ends when  $s'$  is a terminal state. In this paper, we are interested in episodic problems (ex: an episode ends once the taxi driver gets a customer).

We now describe three approaches that are of relevance to work described in this paper.

### 3.1 Q-Learning

One of the most popular approaches for RL is Q-learning Watkins and Dayan [1992], where the Q function is represented as a table (and initialised to arbitrary fixed values) with an entry in the table for each state and action combination. Q-values are updated based on each experience given by  $(s, a, s', r)$ :

$$Q(s, a) \leftarrow Q(s, a) + \alpha[r + \gamma * \max_{a'} Q(s', a') - Q(s, a)] \quad (1)$$

Where  $\alpha$  is the learning rate and  $\gamma$  is the discount factor. To ensure a good explore-exploit tradeoff, an  $\epsilon$ -greedy policy is typically employed. Q-learning is guaranteed to converge to the optimal solution for stationary domains Watkins and Dayan [1992].

### 3.2 Deep Q-Networks (DQN)

Instead of a tabular representation for Q function employed by Q-Learning, the DQN approach Mnih et al. [2015] employs a deep network to represent the Q function. Unlike with the tabular representation that is exhaustive (stores Q-value for every state, action pair), a deep network predicts Q-values based on similarities in state and action features. This deep network for Q-values is parameterised by a set of parameters,  $\theta$  and the goal is to learn values for  $\theta$  so that a good Q-function is learnt.

We learn  $\theta$  using an iterative approach that employs gradient descent on the loss function. Specifically, the loss function at each iteration is defined as follows:

$$\mathcal{L}_\theta = \mathbb{E}_{(e \sim U(\mathcal{J}))} [(y^{DQN} - Q(s, a; \theta))^2]$$

where  $y^{DQN} = r + \gamma \max_{a'} Q(s', a'; \theta^-)$  is the target value computed by a target network parameterised by previous set of parameters,  $\theta^-$ . Parameters  $\theta^-$  are frozen for some time while updating the current parameters  $\theta$ . To ensure independence across experiences (a key property required by Deep Learning methods to ensure effective learning), this approach maintains a replay memory  $\mathcal{J}$  and then samples experiences from that replay memory. Like with traditional Q-Learning, DQN also typically employs an  $\epsilon$ -greedy policy.

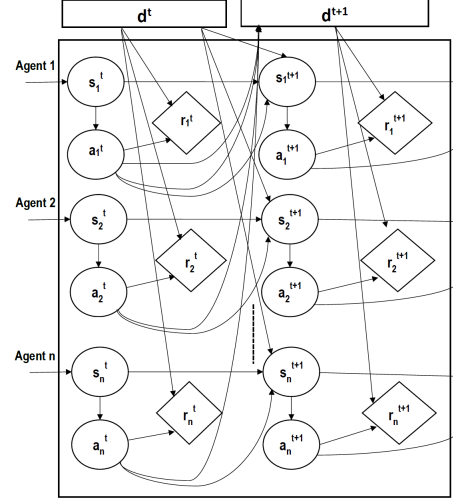


Figure 1: A DBN depicting relationship between transitions and rewards on agent population density distribution  $\mathbf{d}^t$ .

### 3.3 Advantage Actor Critic (A2C)

DQN learns the Q-function and then computes policy from the learnt Q-function. A2C is a policy gradient method that directly learns the policy while ensuring that the expected value is maximized. To achieve this, A2C employs two deep networks, a policy network to learn policy,  $\pi(a|s; \theta_p)$  parameterized by  $\theta_p$  and a value network to learn value function of the computed policy,  $V^\pi(s; \theta_v)$  parameterized by  $\theta_v$ .

The policy network parameters are updated based on the policy loss, which in turn is based on the advantage associated with the value function. Formally, the policy loss is given by:

$$\mathcal{L}_{\theta_p} = \nabla_{\theta_p} \log \pi(a|s; \theta_p) A(s, a; \theta_v)$$

where

$$A(s, a; \theta_v) = \sum_{i=0}^{i=k-1} \gamma^i r_{t+i} + \gamma^k V(s_k; \theta_v) - V(s; \theta_v) \quad (2)$$

The first term in equation 2 is the  $k$ -step (or till the end of the episode) discounted reward following the current policy and using a discount factor  $\gamma$ .

## 4 Anonymous Multi-Agent Reinforcement Learning (AyMARL)

The generalization of the Markov Decision Process (MDP) to the multi-agent case with special interested agents is the stochastic game model Shapley [1953]. The underlying model in AyMARL is a specialization of the stochastic game model that considers interaction

anonymity and is represented using the Dynamic Bayes Network (DBN) in Figure 1:

$$\langle \mathcal{N}, \mathcal{S}, \{\mathcal{A}_i\}_{i \in \mathcal{N}}, \mathcal{T}, \{\mathcal{R}_i\}_{i \in \mathcal{N}} \rangle$$

$\mathcal{N}$  is the number of agents.  $\mathcal{S}$  is the set of environment states that is factored over individual agent states in MSMPs. For instance in the taxi problem of interest, a environment state  $\mathbf{s}$  is the vector of locations (zone) of all agents, i.e.,  $\mathbf{s} \in \mathcal{S} = (z_1, \dots, z_i, \dots, z_{\mathcal{N}})$ .  $\mathcal{A}_i$  is the action set of each individual agent. In case of the taxi problem, an action  $a_i \in \mathcal{A}_i$  represents the zone to move to if there is no customer on board.

$\mathcal{T}$  is the transitional probability of environment states given joint actions:

$$p(\mathbf{s}' | \mathbf{s}, \mathbf{a}) = \mathcal{T}(\mathbf{s}, \mathbf{a}, \mathbf{s}') = \mathcal{T}(\mathbf{s}, (a_1, \dots, a_{\mathcal{N}}), \mathbf{s}')$$

Given the agent state distribution,  $\mathbf{d}$ , agent transitions are independent in AyMARL, i.e.:

$$= \prod_i \mathcal{T}_i(z_i, a_i, z'_i, d_{z_i}(\mathbf{s})) \quad (3)$$

$$= \mathcal{T}_i(z_i, a_i, z'_i, d_{z_i}(\mathbf{s})) \cdot p(\mathbf{d}'(\mathbf{s}'_{-i}) | \mathbf{d}(\mathbf{s}), \mathbf{a}_{-i}) \quad (4)$$

where  $d_{z_i}(\mathbf{s}) = \#_{z_i}(\mathbf{s})$ , is the number of agents in zone  $z_i$  in joint state  $\mathbf{s}$ .

$\mathcal{R}_i(\mathbf{s}, a_i)$  is the reward obtained by agent  $i$  if joint state is  $\mathbf{s}$ . In AyMARL, it is given by  $\mathcal{R}_i(z_i, a_i, d_{z_i}(\mathbf{s}))$ .

**Extensions to AyMARL:** For purposes of explainability, we will employ the model described above in the rest of the paper. However, we wish to highlight that multiple extensions are feasible for AyMARL and can be readily addressed with minor modifications to learning approaches. First extension is the dependence of transition and reward on  $\mathbf{d}(\mathbf{s})$  (or some subset of  $\mathbf{d}$  given by  $d_{\{z_j, z_k, \dots\}}(\mathbf{s})$ ) and not just on  $d_{z_i}(\mathbf{s})$ . A second extension is considering dependence of transition and reward on agent state, action distributions and not just on agent state distributions. That is to say, reward and transitions are dependent on  $d_{z_i, a_i}(\mathbf{s}, \mathbf{a})$  or more generally  $\mathbf{d}(\mathbf{s}, \mathbf{a})$ .

## 5 Independent Learning in AyMARL

Due to the independent and selfish nature of agents coupled with the lack of access to specific state and action information of other agents, we focus on independent learning approaches for AyMARL problems. We adapt leading single agent RL approaches to learn in the presence of other learning agents for AyMARL settings.

To explain the key idea of this paper, we work through the Q-function expression for a given agent  $i$  in stochastic

games:

$$\begin{aligned} Q_i(\mathbf{s}, \mathbf{a}) &= \sum_{\mathbf{s}', r_i} p(\mathbf{s}', r_i | \mathbf{s}, \mathbf{a}) \cdot \left[ r_i + \gamma * \max_{\mathbf{a}'} Q_i(\mathbf{s}', \mathbf{a}') \right] \\ &= \sum_{\mathbf{s}', r_i} p(\mathbf{s}' | \mathbf{s}, \mathbf{a}) \cdot p(r_i | \mathbf{s}, \mathbf{a}) \cdot \left[ r_i + \gamma * \max_{\mathbf{a}'} Q_i(\mathbf{s}', \mathbf{a}') \right] \end{aligned}$$

From Equation 4, we have

$$\begin{aligned} &= \sum_{\mathbf{s}', r_i} \mathcal{T}_i(z_i, a_i, z'_i, d_{z_i}(\mathbf{s})) \cdot p(\mathbf{d}'(\mathbf{s}'_{-i}) | \mathbf{d}(\mathbf{s}), \mathbf{a}) \\ &\cdot p(r_i | z_i, a_i, d_{z_i}(\mathbf{s})) \cdot \left[ r_i + \gamma * \max_{\mathbf{a}'} Q_i(\mathbf{s}', \mathbf{a}') \right] \quad (5) \end{aligned}$$

In MSMPs of interest, individual agents (e.g., taxis, truck drivers) do not get access <sup>1</sup> to the joint state  $\mathbf{s}$ , or joint action  $\mathbf{a}$ . Therefore, we modify the above expression for independent learning as follows:

$$\begin{aligned} Q_i(z_i, d_{z_i}(\mathbf{s}), a_i) &= \sum_{\mathbf{s}', r_i} \mathcal{T}_i(z_i, \dots) \cdot p(\mathbf{d}'(\mathbf{s}'_{-i}) | d_{z_i}(\mathbf{s}), a_i) \\ &\cdot p(r_i | \dots) \cdot \left[ r_i + \gamma * \max_{\mathbf{a}'} Q_i(z'_i, d'_{z'_i}(\mathbf{s}'), a'_i) \right] \end{aligned}$$

where  $\mathcal{T}_i(z_i, \dots) = \mathcal{T}_i(z_i, a_i, z'_i, d_{z_i}(\mathbf{s}))$  and  $p(r_i | \dots) = p(r_i | z_i, a_i, d_{z_i}(\mathbf{s}))$ .

Due to dependence on other agents, the term  $p(\mathbf{d}'(\mathbf{s}'_{-i}) | d_{z_i}(\mathbf{s}), a_i)$  is non-stationary in the learning problem of agent  $i$  and hence is difficult to predict or control. We can either marginalize the expression in Equation 5 with respect to joint state and joint actions or improve the accuracy of computing  $p(\mathbf{d}'(\mathbf{s}'_{-i}) | d_{z_i}(\mathbf{s}), a_i)$  when doing independent learning. Since prior probabilities of marginalization are dependent on policies of other agents, the overall learning process becomes quite cumbersome. Therefore, we focus on improving accuracy in prediction of  $p(\mathbf{d}'(\mathbf{s}'_{-i}) | d_{z_i}(\mathbf{s}), a_i)$ .

The key idea of this paper is therefore to maximize entropy of predicted future agent state distribution,  $\mathbf{d}'(\mathbf{s}'_{-i})$  (or equivalently  $\mathbf{d}'(\mathbf{s}')$ ) along with that of the Q-function for agent  $i$ . Intuitively, such an approach is extremely promising due to the following reasons:

- *Principle of maximum entropy* : According to the principle of maximum entropy Jaynes [1957], the probability distribution that best represents the current state of knowledge is the one with the highest entropy, in the context of precisely stated prior data. Entropy is maximized subject to satisfying the expected value constraints with respect to observed past data. Specifically, Past observations on  $d'(z'_i)$  place the expected value constraints required on the overall distribution  $\mathbf{d}'(\mathbf{s}')$ .
- *Controlling the non-stationarity*: The domains mentioned in Section 2 have reward values that decrease

<sup>1</sup>centralized entities like Uber that perform the matching typically decide the access for individual drivers.

with increasing number of agents. Due to this property and based on domain knowledge, it is beneficial for agents to spread out across zones with demand rather than assemble only in zones with high demand. In other words, current agent takes an action that will maximize the entropy of (normalized)  $\mathbf{d}'(\mathbf{s}')$ .

- *Homogeneity in experience*: In MSMPs, there is homogeneity in learning experiences of agents because the rewards (revenue model) and transitions (allocation of demand to individuals) are determined consistently by a centralized entity (e.g., Uber, Deliveroo).

Given their ability to handle non-stationarity better than normal Q-learning, we implement this idea in the context of DQN Mnih et al. [2015] and A2C Mnih et al. [2016]. It should be noted that an experience  $e$  in AyMARL is more extensive than in normal RL and is given by  $(z_i, a_i, d_{z_i}(\mathbf{s}), r_i, z'_i, d'_{z'_i}(\mathbf{s}'))$ .

### 5.1 Density Entropy based Deep Q-Networks, DE-DQN

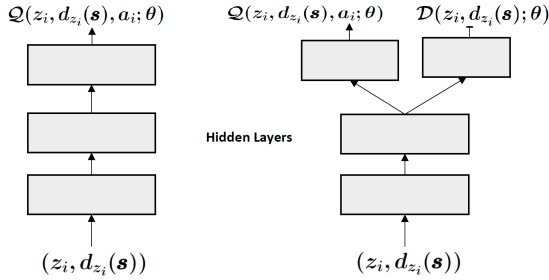


Figure 2: DQN and DE-DQN networks

We now operationalize our general idea of maximizing entropy for the predicted future agent state distribution,  $\mathbf{d}'(\mathbf{s}')$  alongside the expected reward in the context of Deep Q-Networks. We refer to entropy for the predicted future agent state distribution as density entropy.

Since principle of maximum entropy Jaynes [1957] forms the basis for maximizing entropy in our case, we build our approach on applying principle of maximum entropy to DQN. There are two key considerations: (a) maximizing entropy; (b) ensuring expected value of the computed distribution follows the expected value of observed samples. We achieve these considerations using two steps:

- *Including entropy in the Q-loss*: This step enables us to maximize entropy alongside expected reward. The Q-loss,  $\mathcal{L}_\theta^Q$  is updated to include entropy of the predicted agent density for the next step, i.e.,  $\mathbf{d}'(\mathbf{s}')$ . Extending from the description of DQN in Section 3.2,  $\mathcal{L}_\theta^Q$  is

given by:

$$\mathcal{L}_\theta^Q = \mathbb{E}_{(e \sim U(\mathcal{J}))} \left[ \left( y^{DE-DQN} - Q(z_i, d_{z_i}(\mathbf{s}), a_i; \theta) \right)^2 \right]$$

To maximize entropy of  $\mathbf{d}'(\mathbf{s}')$  alongside the expected reward, the target value is:

$$y^{DE-DQN} = r + \beta \mathcal{H}_{\mathbf{d}'(\mathbf{s}')} + \gamma \max_{a'_i} Q(z'_i, d_{z'_i}(\mathbf{s}'), a'_i; \theta^-)$$

- *Introduce a new density loss,  $\mathcal{L}_\theta^D$* : This step enables us to minimize loss in prediction of agent density for the next step. Specifically, by minimizing loss we ensure that density entropy maximization occurs subject to observed samples of  $\mathbf{d}'(\mathbf{s}')$ . The independent learner agent gets to observe only the local density,  $d_{z'_i}(\mathbf{s}')$  and not the full density distribution  $\mathbf{d}'(\mathbf{s}')$ . Hence, we compute MSE loss,  $\mathcal{L}_\theta^D$  for the local observation.

$$\mathcal{L}_\theta^D = \mathbb{E}_{(e \sim U(\mathcal{J}))} [(d_{z'_i}(\mathbf{s}') - \mathcal{D}(d_{z'_i}(\mathbf{s}') | z_i, d_{z_i}(\mathbf{s}); \theta))^2] \quad (6)$$

$\mathcal{D}(\cdot | z_i, d_{z_i}(\mathbf{s}); \theta)$  is the density prediction. To compute the density distribution (which sums up to 1) and to compute density entropy,  $\mathcal{H}_{\mathbf{d}'(\mathbf{s}')}$  we apply softmax function to the density prediction and determine  $\mathcal{D}^{softmax}(\cdot | z_i, d_{z_i}(\mathbf{s}); \theta)$ . The density entropy can be computed as follows

$$\mathcal{H}_{\mathbf{d}'(\mathbf{s}')} = - \sum_{z'_i \in \mathbf{s}'} \mathcal{D}^{softmax}(d_{z'_i}(\mathbf{s}') | z_i, d_{z_i}(\mathbf{s}); \theta) \log(\mathcal{D}^{softmax}(d_{z'_i}(\mathbf{s}') | z_i, d_{z_i}(\mathbf{s}); \theta)) \quad (7)$$

DE-DQN optimizes a single combined loss with respect to the joint parameter  $\theta$ ,  $\mathcal{L}_\theta = \mathcal{L}_\theta^Q + \lambda \mathcal{L}_\theta^D$ .  $\lambda$  is the weight term used for the density prediction loss. Figure 2 shows how DQN can be modified to DE-DQN. In algorithm 1 we show steps of DE-DQN. Network parameters are updated after every  $I_{update}$  steps.  $I_{target}$  is the number of fixed steps after which target network parameter is updated and replay memory  $\mathcal{J}$  is reset after every  $I_{replay}$  steps.

---

**Algorithm 1** DE-DQN
 

---

- 1: Initialize replay memory  $\mathcal{J}$
  - 2: Initialize counter  $T = 0$
  - 3: Initialize action-value function  $Q(z_i, d_{z_i}(\mathbf{s}), a_i; \theta)$  and population density distribution function  $\mathcal{D}(\cdot|z_i, d_{z_i}(\mathbf{s}); \theta)$  with random weight  $\theta$
  - 4: Initialize network gradient  $d\theta \leftarrow 0$
  - 5: Initialize target network parameters  $\theta^- = \theta$
  - 6: **repeat**
  - 7:   Clear gradient  $d\theta \leftarrow 0$
  - 8:    $T \leftarrow T + 1$
  - 9:   Take action  $a_i$  using  $\epsilon$ -greedy policy according to  $Q(z_i, d_{z_i}(\mathbf{s})), a_i; \theta$  and observe  $r_i, z'_i$  and  $d_{z'_i}(\mathbf{s}')$
  - 10:   Store transition  $\langle z_i, d_{z_i}(\mathbf{s}), a_i, r_i, z'_i, d_{z'_i}(\mathbf{s}') \rangle$  to the replay memory.
  - 11:   **if**  $T \bmod I_{update} == 0$  **then**
  - 12:     Sample batch of transitions from the replay memory
  - 13:     Compute  $\mathcal{L}_\theta^Q, \mathcal{L}_\theta^D$  and overall network loss  $\mathcal{L}_\theta$
  - 14:     Accumulate gradients wrt  $\theta : d\theta \leftarrow d\theta + \nabla_\theta \mathcal{L}_\theta$
  - 15:     Update  $\theta$  based on  $d\theta$
  - 16:     **if**  $T \bmod I_{target} == 0$  **then**
  - 17:       Update target network parameter,  $\theta^- \leftarrow \theta$
  - 18:     **if**  $T \bmod I_{replay} == 0$  **then**
  - 19:       Reset replay memory
  - 20: **until**  $T > T_{max}$
- 

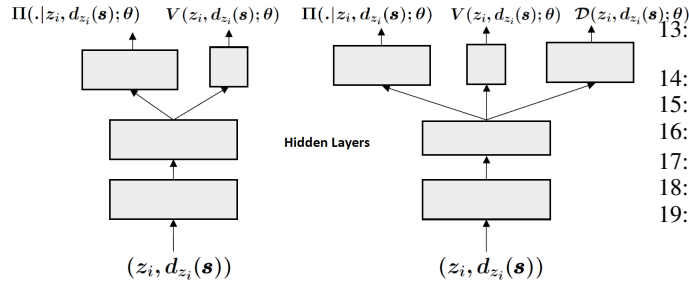
**5.2 Density Entropy based A2C, DE-A2C**


Figure 3: A2C and DE-A2C networks

Figure 3 depicts how A2C network can be modified to DE-A2C network. DE-A2C maintains a policy network  $\pi(\cdot|z_i, a_i, d_{z_i}(\mathbf{s}); \theta_p)$  parameterised by  $\theta_p$  and a value network parameterised by  $\theta_v$ . Value network maintains a value function output  $V(z_i, d_{z_i}(\mathbf{s}); \theta_v)$  and a density prediction output  $\mathcal{D}(z_i, d_{z_i}(\mathbf{s}); \theta_v)$ .  $R$  is the episodic return (or  $k$ -step return) from the experience. While computing the value function loss  $\mathcal{L}_{\theta_v}^V$ , density entropy is added to  $R$  as follows

$$\mathcal{L}_{\theta_v}^V = \mathbb{E}_{(e \sim U(\mathcal{J}))} [(R + \beta \mathcal{H}_{\mathbf{a}'(s')} - V(z_i, d_{z_i}(\mathbf{s}); \theta_v))^2]$$

Density prediction loss  $\mathcal{L}_{\theta_v}^D$  can be computed as given in equations 6. The value network loss  $\mathcal{L}_{\theta_v}$  is the combination of value loss and density loss,  $\mathcal{L}_{\theta_v} = \mathcal{L}_{\theta_v}^V + \lambda \mathcal{L}_{\theta_v}^D$ . Similarly, the policy network loss is computed by adding

the density entropy to the advantage term as follows.

$$\mathcal{L}_{\theta_p} = \mathbb{E}_{(e \sim U(\mathcal{J}))} [\nabla_{\theta_p} \log \pi(a_i | z_i, d_{z_i}(\mathbf{s}); \theta_p) (R + \beta \mathcal{H}_{\mathbf{a}'(s')} - V(z_i, d_{z_i}(\mathbf{s}); \theta_v))]$$

Algorithm 2 shows the steps for DE-A2C. We estimate the value based on  $k$ -step return (or till the end of the episode, whichever comes first). A small replay memory is also used which contains episodes generated from  $\pi(\cdot|z_i, d_{z_i}(\mathbf{s}); \theta_p)$  and replay memory is reset after every update of  $\theta_p$ .

---

**Algorithm 2** DE-A2C
 

---

- 1: Initialize replay memory
  - 2: Initialize counter  $T = 0$
  - 3: Initialize value function  $V(z_i, d_{z_i}(\mathbf{s}); \theta_v)$  with random weight  $\theta_v$
  - 4: Initialize policy function  $\pi(\cdot|z_i, d_{z_i}(\mathbf{s}); \theta_p)$  with random weight  $\theta_p$
  - 5: Initialize network gradients  $d\theta_p \leftarrow 0$  and  $d\theta_v \leftarrow 0$
  - 6: **repeat**
  - 7:   Clear gradients  $d\theta_p \leftarrow 0$  and  $d\theta_v \leftarrow 0$
  - 8:    $t_{start} \leftarrow T$
  - 9:   **repeat**
  - 10:     Take action  $a_i$  according to policy  $\pi(\cdot|z_i, d_{z_i}(\mathbf{s}); \theta_p)$  and observe  $r_i, z'_i$  and  $d_{z'_i}(\mathbf{s}')$
  - 11:      $T \leftarrow T + 1$
  - 12:     **until** terminal or  $T - t_{start} == k$
  - 13:      $R = \begin{cases} 0 & \text{if } \mathbf{s}' \text{ is terminal} \\ V(z'_i, d_{z'_i}(\mathbf{s}'); \theta_v) & \text{otherwise} \end{cases}$
  - 14:     **for**  $i \in T - 1, \dots, t_{start}$  **do**
  - 15:        $R \leftarrow r_i + \gamma R$
  - 16:       add  $\langle z_i, d_{z_i}(\mathbf{s}), a_i, R, z'_i, d_{z'_i}(\mathbf{s}') \rangle$  to  $\mathcal{J}$
  - 17:     **if**  $T \bmod I_{update} == 0$  **then**
  - 18:       sample batch of experience from  $\mathcal{J}$
  - 19:       Accumulate gradients wrt  $\theta_p$  :  

$$d\theta_p \leftarrow \nabla_{\theta_p} \log \pi(a_i | z_i, a_i, d_{z_i}(\mathbf{s}); \theta_p) (R + \beta \mathcal{H}_{\mathbf{a}'(s')} - V(z_i, d_{z_i}(\mathbf{s}); \theta_v)) +$$
  - 20:       Accumulate gradients wrt  $\theta_v$  :  $d\theta_v \leftarrow d\theta_v + \nabla_{\theta_v} \mathcal{L}_{\theta_v}$
  - 21:       Update  $\theta_p$  and  $\theta_v$  using  $d\theta_p$  and  $d\theta_v$  respectively.
  - 22:       Clear replay memory  $\mathcal{J}$ .
  - 23: **until**  $T > T_{max}$
- 

**6 Experiments**

In this section, we demonstrate that our approaches which employ density entropy alongside Q-function or value function are able to outperform leading independent RL approaches (DQN, A2C, Q-Learning). First, we provide results on a taxi simulator (described in Section 2) that is validated from a real dataset. Second, we provide results on a synthetic online to offline matching simulator (that is representative of problems in Section 2) under various conditions. Finally, we provide results on an anti-congestion domain (i.e., rewards increase when more

agents congregate in a state), where we minimize density entropy.

**Taxi Simulator:** Figure 4 shows the map of Singapore where road network is divided into zones. First, based on the GPS data of taxi-fleet, we divided the map of Singapore into 111 zones. Then we used the real world data to compute the demand between two zones and the time taken to travel between the zones. Since we focus on independent learners, our learning is very scalable. However, simulating thousands of learning agents at the same time requires extensive computer resources and with the academic resources available, we could not perform a simulation with thousands of agents. Hence, we computed proportional demand for 100 agents and simulated for 100 agents.

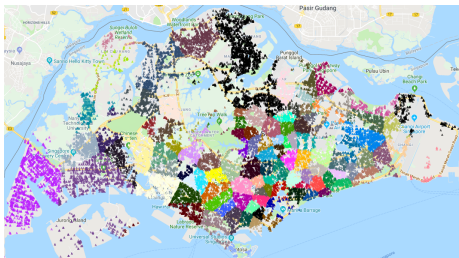


Figure 4: Road network of Singapore divided into zones.

**Synthetic Online to Offline Service Simulator:** We generated synthetic data to simulate various combinations of demand and supply scenarios in a generic online to offline service settings described in Section 2. We used grid world and each grid is treated as a zone. Demands are generated with a *time-to-live* value and the demand expires if it is not served within *time-to-live* time periods. Furthermore, to emulate the real-world jobs, the revenues are generated based on distance of the trip (distance between the origin and destination grids). There are multiple agents in the domain and they learn to select next zones to move to such that their long term payoff is maximized. At every time step, the simulator assigns a trip to the agents based on the agent population density at the zone. In our experiments, we make a realistic assumption that agents do not take action at every time step and they can go to any zone from any zone and time taken to travel between zones is proportional to the shortest distance between the grids. The revenue of an agent can be affected by various features of the taxi domain.

- Demand-to-Agent Ratio (DAR): This is the average number of customers per time step per agent.
- Trip pattern: The average length of trips can be uniform for all the grids or there can be few grids which always get longer trips (for ex. airports which are

usually outside the city) whereas few grids get relatively shorter trips (city center).

- Demand pattern: The demand can be uniformly spread across all the grids (dispersed demand) or there might be few grids where high demand is present and few grids where there is no demand (concentrated demands)
- Demand arrival rate: The Poisson arrival rate of demand can be either homogeneous (static arrival rate) or non-homogeneous (dynamic arrival rate)

We perform experiments with various combinations of these features.

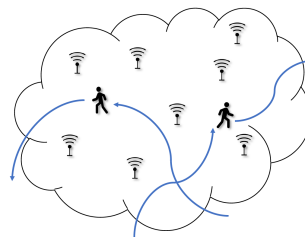


Figure 5: Sensor network.

**Sensor Network Simulator:** Figure 5 represents an example sensor network domain with 8 sensors and 2 targets. We simulated the domain using a grid world where sensors are present at all the inner nodes of the grid. Targets follow fixed paths but their movement is probabilistic. The sensors can align to one of the four adjoining grids and they receive payoff for successfully tracking a target. The payoff received increases with number of sensors tracking a target and each sensor tracking the same target gets equal payoff. The task for each agent is to learn to align in such a way that their expected payoff is maximized.

## 6.1 Hyperparameters

For DQN algorithms we used Adam optimizer [Kingma and Ba, 2014] with a learning rate of  $1e-4$ , whereas for A2C algorithms we used RMSprop optimizer [Tieleman and Hinton, 2012] with learning rate of  $1e-5$  for policy network and  $1e-4$  for value network. Two hidden layers were used with 128 nodes per layer. Density entropy regularizer  $\beta$  was set to  $1e-2$ , whereas weightage of D-loss  $\lambda$  was set to  $1e3$ . We also used policy entropy regularizer for A2C algorithms and the regularizer was set to  $1e-3$ .

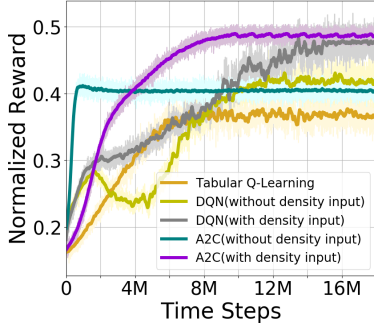


Figure 6: Comparison of tabular Q-learning, standard DQN and standard A2C .

## 7 Experimental results

In this section, we benchmark the performance of our approaches (DE-DQN and DE-A2C) with respect to tabular Q-learning, DQN/A2C without density distribution input and finally DQN/A2C with density distribution input. One evaluation period consists of 1000 (1e3) time steps<sup>2</sup> and revenue of all the agents is reset after every evaluation period. All the graphs plotted in the upcoming sub-sections provide running average of revenue over 100 evaluation periods (1e5 time steps). Unless specified, the number of agents employed was 20. We used one step learning for the sensor network example whereas for taxi domain example we performed episodic learning (an episode starts when the taxi agent starts looking for a trip and ends when a trip is assigned to it).

We evaluated the performance of all learning methods on two key metrics:

- (1) Payoff for each of the individual Independent Learners (ILs) and,
- (2) Average payoff of all the individual Independent Learners (ILs).

### 7.1 Taxi Simulator and Synthetic Online to Offline Services Simulator:

Both these domains are examples of congestion settings where having more agents in a state decreases the payoff. Therefore, we maximize the density entropy. We use DQN and A2C as the baseline algorithms.

**Tabular Q-Learning, Standard DQN and Standard A2C:** Figure 6 shows the comparison between tabular Q-learning; DQN with and without agent density input and A2C with and without agent density input. We used medium demand-to-agent ratio with non-uniform trip pat-

<sup>2</sup>A time step represents a decision and evaluation point in the simulator. From a learner perspective, an episode is typically multiple time steps long.

tern.

We can see that DQN with agent density input and A2C with agent density input perform significantly better than the other three algorithms. Even for other demand we obtained similar results.

**Taxi domain simulated using real-world data set:** First plot in figure 7 provides comparison of average payoff of all the ILs for real world dataset validated taxi simulator. The second plot displays individual payoff received by 100 agents with time where each curve on the plot represents one agent. We can see that both DE-DQN

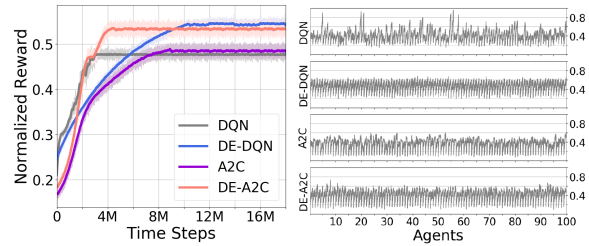


Figure 7: Average reward and individual rewards for real world dataset.

and DE-A2C outperforms their counterpart baseline algorithms. The variance in individual agents' revenue has also decreased for density entropy algorithms.

**Low DAR (Demand-to-Agent Ratio) uniform trip pattern and dispersed demand:** In this case, static demand

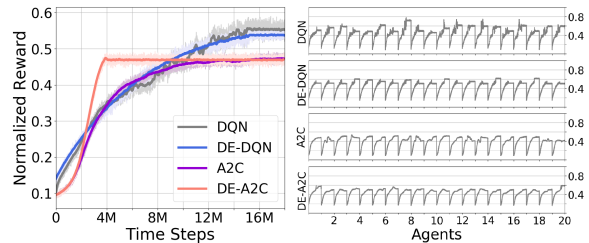


Figure 8: Average reward and individual rewards for low DAR with uniform trip pattern and dispersed demand.

arrival rate was used. The effective demand-to-agent ratio was 0.5. Figure 8 provide the joint and individual normalized rewards obtained by different approaches. Here are the key observations: (1) Both DE-DQN and DE-A2C perform similar to DQN and A2C respectively. This can be attributed to the static nature of the domain in this experimental setup.

(2) DE-DQN, A2C and DE-A2C all provide a reasonably fair distribution of revenues for individual revenues, with DE-DQN providing higher individual revenues.

**Low DAR (Demand-to-Agent Ratio) with non-uniform trip pattern:** For this setup we simulated 50

agents and demand-to-agent ratio was set to 0.3. We can

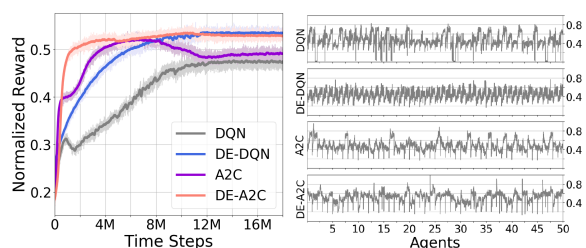


Figure 9: Average reward and individual rewards for synthetic dataset.

see in figure 9 that when we increased the complexity of the experimental setup in terms of trip pattern, DE-DQN and DE-A2C start performing better than DQN and A2C respectively.

**Medium DAR with concentrated demand:** In this setting, there were few grids with high demand whereas remaining grids did not have any demand and the overall demand-to-agent ratio was 0.8. The poisson arrival rate was homogeneous and uniform trip pattern was used. Here are the key observations: (1) Figure 10 shows that both DE-A2C performs better than other algorithms, with DE-DQN providing the second best performance. (2) DQN, DE-DQN and A2C provide reasonably fair distribution of individual revenues, with DE-A2C providing slightly uneven distribution of revenues for individual agents.

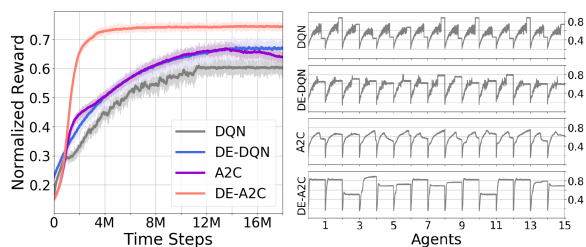


Figure 10: Average reward and individual rewards for medium DAR with concentrated demand pattern.

**Medium DAR with non-uniform trip patterns:** In this setting, we employed a demand-to-agent ratio of 0.8 and non-uniform trip patterns. Arrival of demand was generated based on homogeneous Poisson rates and to generate a non-uniform trip pattern, we associated each grid cell with a maximum range for destination grids for trips originating from the grid cell. Here are the key observations: (1) We observed that as we increase complexity of demand pattern, the performance of DE-DQN starts improving with respect to DQN. First plot in figure 11 compares the performances of all the algorithms. (2) Second plot in figure 11 shows that DE-DQN and A2C

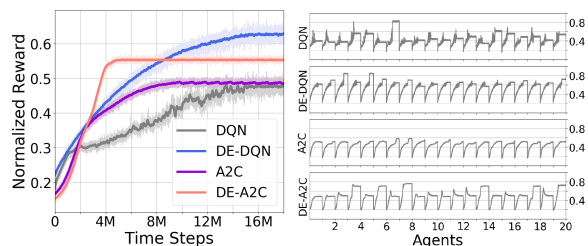


Figure 11: Average reward and individual rewards for medium DAR with non-uniform trip pattern.

provide low variance across individual revenues.

**High DAR with non-uniform trip patterns:** We gener-

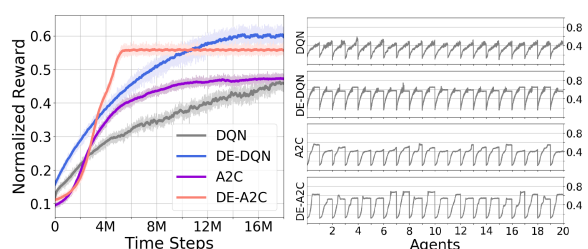


Figure 12: Average reward and individual rewards for high DAR with non-uniform trip patterns.

ated high demand-to-agent ratio (1.2) in this setting. Once again, we observe that in figure 12, DE-DQN provides better joint revenue and less variance across individual agent revenues.

**Medium DAR with dynamic demand arrival rate:** To simulate peak and off-peak hours we divided the evaluation period (1e3 time steps) into three parts. The demand for the first and third part is generated based on low demand-to-agent ratio (0.6) and for the second part it is generated using high demand-to-agent ratio (1.2).

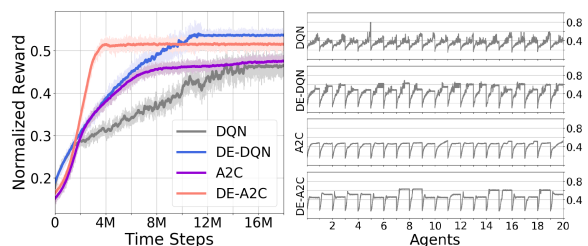


Figure 13: Medium DAR with dynamic demand arrival rate.

Figure 13 shows that the performances are similar to what we have seen for other settings, with DE-DQN providing higher values while having lower variance across individual agents.

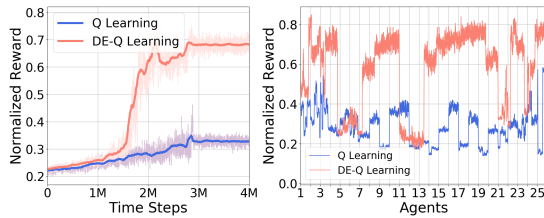


Figure 14: Average and individual rewards for sensor network example.

**Sensor Network** As sensor network is an anti-congestion domain (i.e., payoff is higher if more sensors track a target location), we minimize the density entropy. To compute density entropy based on local observation of an IL, we maintained a sliding window of number of agents observed for past 100 time steps. Using this list, we estimate agent density distribution of neighbour agents for each IL and compute entropy. For this domain, Q-learning updated with density entropy was able to perform extremely well, so we do not consider DQN and A2C.

We use Q-Learning as baseline algorithm for this experiment. Q-Learning is extended to DE-Q-Learning by deducting the entropy of the estimated density distribution from the observed payoff. Figure 14 shows experimental results for a sensor network with 6 targets and 25 sensors. Here are the key conclusions:

- The average value of DE-Q Learning was significantly better than normal Q-learning.
- Unlike with the congestion domains, the position of a sensor determines the reward that can be obtained. Hence, this domain is inherently not fair to all sensors and this is reflected in the difference. However, the agents that are in good positions all obtained close to equal values.

**Summary of Results** Our key idea of maximizing (or minimizing) density entropy is extremely effective in Ay-MARL settings both with respect to overall value of all agents and fairness in values obtained by individual agents (where relevant). We have validated this on three different simulators.

## References

Busoniu, L., Babuska, R., and De Schutter, B. (2008). A comprehensive survey of multiagent reinforcement learning. *IEEE Trans. Systems, Man, and Cybernetics, Part C*.

Foerster, J., Assael, Y., de Freitas, N., and Whiteson, S. (2016). Learning to communicate with deep multi-agent reinforcement learning. In *NIPS*.

Hausknecht, M. and Stone, P. (2015). Deep reinforcement learning in parameterized action space. *arXiv preprint arXiv:1511.04143*.

Jaynes, E. T. (1957). Information theory and statistical mechanics. *Physical review*, 106(4):620.

Kingma, D. P. and Ba, J. (2014). Adam: A method for stochastic optimization. *arXiv preprint arXiv:1412.6980*.

Mnih, V., Badia, A. P., Mirza, M., Graves, A., Lillicrap, T., Harley, T., Silver, D., and Kavukcuoglu, K. (2016). Asynchronous methods for deep reinforcement learning. In *ICML*.

Mnih, V., Kavukcuoglu, K., Silver, D., Rusu, A. A., Veness, J., Bellemare, M. G., Graves, A., Riedmiller, M., Fidjeland, A. K., Ostrovski, G., et al. (2015). Human-level control through deep reinforcement learning. *Nature*.

Nguyen, D. T., Kumar, A., and Lau, H. C. (2017a). Collective multiagent sequential decision making under uncertainty.

Nguyen, D. T., Kumar, A., and Lau, H. C. (2017b). Policy gradient with value function approximation for collective multiagent planning. In *NIPS*.

Perolat, J., Leibo, J. Z., Zambaldi, V., Beattie, C., Tuyls, K., and Graepel, T. (2017). A multi-agent reinforcement learning model of common-pool resource appropriation. In *NIPS*.

Shapley, L. S. (1953). Stochastic games. *Proceedings of the national academy of sciences*.

Silver, D., Schrittwieser, J., Simonyan, K., Antonoglou, I., Huang, A., Guez, A., Hubert, T., Baker, L., Lai, M., Bolton, A., et al. (2017). Mastering the game of go without human knowledge. *Nature*.

Tan, M. (1993). Multi-agent reinforcement learning: Independent vs. cooperative agents. In *ICML*.

Tieleman, T. and Hinton, G. (2012). Lecture 6.5-rmsprop: Divide the gradient by a running average of its recent magnitude. *COURSERA: Neural networks for machine learning*, 4(2):26–31.

Varakantham, P., Adulyasak, Y., and Jaillet, P. (2014). Decentralized stochastic planning with anonymity in interactions. In *AAAI*.

Varakantham, P., Cheng, S.-F., Gordon, G., and Ahmed, A. (2012). Decision support for agent populations in uncertain and congested environments. In *AAAI*.

Verma, T., Varakantham, P., Kraus, S., and Lau, H. C. (2017). Augmenting decisions of taxi drivers through reinforcement learning for improving revenues. In *ICAPS*.

Watkins, C. J. and Dayan, P. (1992). Q-learning. *Machine learning*, 8(3-4):279–292.